



Impact of the assimilation of water vapour isotopologues on diabatic heating and precipitation in the tropics

Farahnaz Khosrawi¹, Kinya Toride², Kei Yoshimura², Christopher J. Diekmann^{1,*}, Benjamin Ertl^{1,3}, Frank Hase¹, and Matthias Schneider¹

¹Institute of Meteorology and Climate Research (IMK), Karlsruhe Institute of Technology, Karlsruhe, Germany

²Institute of Industrial Science, University of Tokyo, Chiba, Japan

³Steinbuch Centre for Computing (SCC), Karlsruhe Institute of Technology, Karlsruhe, Germany

*now at: Telespazio Germany GmbH, Darmstadt, Germany

Correspondence: Farahnaz Khosrawi (farahnaz.khosrawi@kit.edu)

Abstract. The strong coupling between atmospheric circulation, moisture pathways and atmospheric diabatic heating is responsible for most climate feedback mechanisms and controls the evolution of severe weather events. However, diabatic heating rates obtained from current meteorological reanalysis show significant inconsistencies. Here, we theoretically assess with an Observation System Simulation Experiment (OSSE) the potential of the Multi-platform remote Sensing of Isotopologues for investigating the Cycle of Atmospheric water (MUSICA) Infrared Atmospheric Sounding interferometer (IASI) mid-tropospheric water isotopologue data for constraining uncertainties in meteorological analysis fields. For this purpose, we use the Isotope-incorporated General Spectral Model (IsoGSM) together with a Local Ensemble Transform Kalman Filter (LETKF) and assimilate synthetic MUSICA IASI water vapour isotopologue observations. We perform four ensemble simulations, three where synthetic IASI isotopologue and humidity data are assimilated and another one where no observational data at all are assimilated. By comparing the ensemble simulations with data assimilation with water isotopologues to the one without any data assimilation we can, in contrast to the former study by Toride et al. (2021) where additionally conventional observations were considered, assess the direct impact of the IASI δD and water vapour data on the meteorological variables, especially on the heating rates and vertical velocity. The assessment is performed for the tropics in the latitude range from 10°S to 10°N. When the synthetic isotopologue data are assimilated, we derive reduced Root-Mean-Square Deviations (RMSDs) and improved skills with respect to meteorological variables (improvement by about 11–17%). When only IASI δD is assimilated the improvement in vertical velocity and heating rate is minor (up to a few percent) and restricted to the mid-troposphere. However, when water vapour alone or δD is assimilated additionally to water vapour, heating rates and vertical motion can be improved throughout the troposphere. The highest improvements, however, are derived when δD is assimilated additionally to water vapour confirming that water isotopologues hold different aspects of information than water vapour. Thus, in consequence δD offers, especially when assimilated additionally to water vapour, potential for improving diabatic heating and precipitation and thus meteorological analysis, weather forecasts and climate predictions in the tropical regions.



1 Introduction

In the past 40 years, medium-range weather forecasts have undergone significant improvements (Bauer et al., 2015). The improvement in forecast skill is mainly due to improved data assimilation techniques, model dynamics and physics, spatial and temporal model resolution, representation of uncertainties, together with improved observing systems whose measurements can be used for data assimilation. Nevertheless, a correct initialisation and the model used for the creation of the initial conditions are crucial for the quality of the weather forecast (Magnusson et al., 2019).

Meteorological analysis and reanalysis are best guesses of the true state of the atmosphere. Therefore, a high accuracy of these are of great importance for both, the initialisation of weather forecasts and for process analysis and detection and attribution of changes in the climate system (Wright and Fueglistaler, 2013). Diabatic heating is the major driving force of atmospheric circulation on weather and climate time scales. However, diabatic heating rates obtained from current meteorological reanalysis show significant inconsistencies (e.g. Chan and Nigam, 2009; Ling and Zhang, 2013; Wright and Fueglistaler, 2013). This jeopardises the accuracy of both climate predictions and numerical weather prediction. This is mainly indebted to the fact that diabatic heating rates cannot be observed directly. Usually, diabatic heating is diagnosed from the atmospheric circulation (wind and temperature) through the thermodynamic energy equation (Peixoto and Oort, 1992; Chan and Nigam, 2009).

Water isotopologue observations (e.g. H_2O and HDO) assimilated into meteorological reanalysis can make an invaluable contribution since the isotopologue composition depends on the history of phase transition. Stable water isotopologue ratios are sensitive to the phase changes during atmospheric circulation. Therefore, water isotopologues are useful tracers for investigating atmospheric processes, such as large-scale transport (e.g. Yoshimura et al., 2003; Lee et al., 2017; Risi et al., 2012; Dee et al., 2018) and cloud-related processes (e.g. Webster and Heymsfield, 2003; Worden et al., 2007). The relation between atmospheric processes and isotopic information in water vapour and precipitation has therefore been studied intensively (e.g. Yoshimura et al., 2004; Schneider et al., 2016; González et al., 2016; Lacour et al., 2017; Risi et al., 2019). Further, isotopologue observations can provide information that is closely linked to diabatic heating processes (e.g. Lacour et al., 2018; Risi et al., 2020).

In the recent decade, advances in satellite remote sensing techniques have significantly increased the availability of tropospheric water vapour isotopologue observations (Worden et al., 2019; Diekmann et al., 2021; Schneider et al., 2022a). Especially, daily quasi-global water isotope observations can be retrieved from the Infrared Atmospheric Sounding Interferometer (IASI) on the Meteorological Operational Satellite Program (Metop) (Schneider et al., 2016; Diekmann et al., 2021). Although with the upcoming Metop generations high resolution water isotope observations will be available for the next decades, their potential on weather forecasting is still largely unexplored.

First attempts for testing the impact of assimilating water isotopologues into numerical weather and climate models were done by Yoshimura et al. (2014) and Toride et al. (2021). Yoshimura et al. (2014) developed a new data assimilation system using a Local Ensemble Transform Kalman Filter (LETKF) and the Isotope-incorporated Global Spectral Model (IsoGSM). They then applied this assimilation system to an Observation System Simulation Experiment (OSSE) using a synthetic data



set that mimicked water vapour isotope measurements from the Tropospheric Emission Spectrometer (TES), the SCanning Imaging Absorption spectroMeter for Atmospheric CHartographY (SCIAMACHY) and the Global Network of Isotopes in Precipitation (GNIP). Their results showed that not only the water isotopic fields were improved but also the meteorological fields (e.g. temperature, pressure, wind speed).

60 In the study by Toride et al. (2021) the same OSSE was used, but synthetic isotopologue data from the Infrared Atmospheric Sounding interferometer (IASI) were assimilated in addition to conventional non-isotopic observations (as e.g. temperature, winds). Toride et al. (2021) compared in their study three different assimilation experiments, one where only IASI δD was assimilated, a second one where only IASI water vapour was assimilated and a third one where both, IASI water vapour and δD was assimilated. Their results showed that the assimilation of water isotopologues in addition to conventional observations
 65 leads to an improvement of the meteorological fields. Further, they showed that the large-scale atmospheric circulation and the weather forecast could be improved when isotopologues are assimilated. Comparing the three assimilation experiments they found that higher improvements can be derived when additional to conventional observations water vapour instead of δD is assimilated. Further improvements however can be derived when both, IASI water vapour and δD are assimilated together. The results by Toride et al. (2021) showed that the assimilation of water vapour is more efficient in terms of improvement,
 70 but that nevertheless an additional improvement of 3-4 % in skill can be derived when δD is assimilated additional to water vapour, thus confirming that δD holds different aspects of information than water vapor (Yoshimura et al., 2011; Noone, 2012; Galewsky et al., 2016).

Here, we build on the study by Toride et al. (2021) and investigate their latter issue further, namely which information is hold by isotopologues? Especially, we are interested in answering the following question: Can the information stored in water
 75 isotopologues help to improve diabatic heating rates and/or precipitation rates? For that an additional OSSE experiment has been performed in the frame of this study where we assess the direct impact of the IASI isotopologues on the meteorological variables. In this OSSE the IASI water vapour isotopologue data are assimilated alone (without any conventional observations) and then compared to an ensemble simulation where no observations at all are assimilated.

In this study, we focus on the inner tropics ($10^{\circ}S$ to $10^{\circ}N$), to assess the impact of isotopologues on the assimilation in
 80 the region where diabatic heating is strong and where the Walker circulation is found. The Walker circulation is a longitudinal (east-west) circulation pattern consisting of several circulation cells spanning over the entire tropics. Convection and heavy precipitation associated with the rising branches of the Walker Circulation occur over Indonesia and the western Pacific, northern South America, and eastern Africa while sinking air and desert conditions prevail over the eastern equatorial Pacific and west Africa (Peixoto and Oort, 1992; Lau and Yang, 2003; Webster and Chang, 1988).

85 The paper is structured as follows. In Sect. 2 we describe the data and method used. In Sect. 3 we assess the performance of the assimilation experiment with the assimilation of the IASI water vapour isotopologue data on the meteorological analyses, especially on diabatic heating and precipitation in the tropics and for specific longitude regions in the tropics (up/down branches of the Walker circulation). Finally, in Sect. 4 we discuss and in Sect. 5 we summarize and conclude our results.



2 Data and Method

2.1 IsoGSM model and data assimilation

For our assimilation experiments we use the isotope-incorporated Global Spectral Model (IsoGSM). This model is based on the Scripps Experimental Climate Predictions Center's (ECPC) Global Spectral Model (GSM) that has been used by NCEP to perform operational analyses and medium-range forecasts (Kanamitsu et al., 2002). Gaseous forms of stable water isotopes (HDO and H₂¹⁸O) are incorporated as prognostic variables in addition to water vapour into GSM (Yoshimura et al., 2008). Simulations with IsoGSM have been used together and also evaluated with both, ground-based (Schneider et al., 2010; Uemura et al., 2008) and space-borne observations (Frankenberg et al., 2009; Yoshimura et al., 2011) of water isotopologues.

Here, we use IsoGSM ensemble simulations performed with a T62 horizontal resolution ($1.9^\circ \times 2^\circ$, $\sim 200 \times 200$ km) and 28 vertical sigma levels from the surface up to ~ 2.5 hPa. The sea surface and sea ice temperature distribution from the National Centers of Environmental Prediction/Department of Energy Reanalysis 2 (NCEP-DOE, Reanalysis 2) have been used as lower boundary condition. The data assimilation is performed with a Local Ensemble Kalman Transform Filter (LETKF, Hunt et al. (2004, 2007)) which is a parallel-efficient update of the traditional Ensemble Transform Kalman Filter (ETKF, Bishop et al. (2001)). For the data assimilation a relaxation-to-prior spread (RTPS) method (Whitaker and Hamill, 2012) is used with a relaxation parameter of 0.4 to maintain an appropriate ensemble spread and to avoid filter divergence. The horizontal localisation scale is set to be 500 km (influence radius of 1826 km for best assimilation performance). The used ensemble size is 96. This large ensemble size is needed to derive results of satisfying quality as was shown by Toride et al. (2021). A detailed description on the data assimilation with LETKF and IsoGSM is provided in Yoshimura et al. (2014) and Toride et al. (2021).

2.2 Observation System Simulation Experiment

To investigate the potential impact of the assimilation of satellite data an Observation System Simulation Experiment (OSSE) is performed. In an OSSE, a model simulation is regarded as “truth” (“Nature run”) and several data assimilation experiments with synthetic observations derived from the Nature run are conducted that aim to reproduce the Nature run as closely as possible (Schrötte et al., 2020). The synthetic data mocks therefore the data that would be obtained if satellites or ground-based sensors were actually operated (Yoshimura et al., 2014). For the OSSEs performed in this study the characteristics of the Infrared Atmospheric Sounding Interferometer (IASI) δD observations generated by the Multi-platform remote Sensing of Isotopologues for investigating the Cycle of Atmospheric water (MUSICA) IASI retrieval processor are mocked (Schneider and Hase, 2011; Schneider et al., 2016; Diekmann et al., 2021). IASI is a nadir-looking Fourier-transform spectrometer onboard the Meteorological Operation Satellites A and B (MetOp-A and MetOp-B) (Clerbaux et al., 2009).

For generating the synthetic MUSICA IASI data set the spatial coverage and the observational error statistics of the real data are used (Diekmann et al., 2021; Schneider et al., 2022b). IASI measurements are obtained with a horizontal resolution of 12 km (pixel diameter at nadir viewing geometry) for cloud free conditions. IASI δD and H₂O pair distributions are provided twice a day (each about 300 000 points) on a quasi-global scale. The IASI data are spatially resampled to the IsoGSM grid at

one vertical sigma level corresponding to 4.2 km, which is the altitude where IASI δD has the highest sensitivity (Schneider et al., 2016). Our mocked “truth” data set has been derived from an IsoGSM simulation and is used as reference for assessing the impact of our assimilation experiments on the meteorological variables. The synthetic observational data set is then generated by adding Gaussian noise with the actual error statistics of the IASI observations to the Nature run (Toride et al., 2021).

2.3 Experimental set-up

In total four ensemble simulations were performed. Thereby, three OSSEs and one ensemble simulation without any data assimilation were performed to assess the potential impact of the IASI δD and water vapour data on the meteorological fields. In the first OSSE synthetic IASI water isotopologues (δD) are assimilated, in the second OSSE synthetic IASI water vapour (q) observations are assimilated and in the third OSSE synthetic IASI water isotopologue data are assimilated additionally to water vapour ($\delta D+q$). The three OSSEs serve to investigate what impact the assimilation of the IASI δD data alone, the IASI water vapour data alone and both together have on the meteorological fields, e.g. on the diabatic heating rates. Therefore, these three OSSEs are compared to an ensemble simulation without assimilation of any observations. All ensemble simulations consist of an ensemble size of 96.

The Nature run is derived from a free running IsoGSM simulation over two years, covering the time period from 2015 to 2016. The model run was started on 1 June 2015 at 00 UTC. The first year has been discarded as spin-up period to minimize the possibility of the model’s drift. The initial conditions for the 96 ensemble members were taken from the Nature run. The first initialisation was done on 1 June 2016 at 00 UTC and then all other ensemble members were initialised with the following consecutive 6-hour time steps. Therefore, the initial conditions can be considered as being independent from the Nature run, but representing similar climatological conditions. The following two months, thus from 1 July 2016 to 1 September 2016 have then been used as the experimental period and the results of our assimilation experiments are then evaluated for the latter one-month period (1 August to 31 August 2016). An overview over our assimilation experiments is given in Table 1.

The assessment of the idealized assimilation experiment is then done by using each experiments ensemble mean, the mean difference between each ensemble mean of the respective assimilation run and the Nature run, the root-mean-square deviation (RMSD) between each experiments ensemble mean and the Nature run and the RMSD skill. The ensemble mean and the mean

Table 1. Specification of the experiments and assimilation runs used in this study. Checkmarks indicate the variables assimilated in each ensemble simulation.

experiment	assimilation run	ensemble size	IASI δD ($\sigma=0.568$)	IASI q ($\sigma=0.568$)	localization (km)	RTPS
noDAvsDA	noDA	96	-	-	-	-
	IASI_ δD	96	✓	-	500	0.4
	IASI_ q	96	-	✓	500	0.4
	IASI_ $\delta D+q$	96	✓	✓	500	0.4



difference between the assimilation run and the Nature run are calculated by:

$$\bar{x} = \frac{1}{N} \sum_{i=1}^N x_i \quad (1)$$

and

$$MD = \frac{1}{N} \sum_{i=1}^N (x_i - x_{n_i}) \quad (2)$$

150 where N denotes the total number of ensemble members, x is the assessed meteorological variable (e.g. T , u , v) of the assimilation experiment and x_n the respective meteorological variable of the Nature run. The RMSD is generally calculated as follows:

$$RMSD = \sqrt{\frac{1}{N} \sum_{i=1}^N (x_i - x_{n_i})^2} \quad (3)$$

We use in our study the same approach as Toride et al. (2021) and Tada et al. (2021), thus for simplification the ensemble mean
 155 instead of each single ensemble member is used to calculate the RMSD. Therefore, in the MD and RMSD equations (Eq. 2 and 3) instead of x and x_n the mean \bar{x} and \bar{x}_n is used and the sum is taken over time or space, respectively, instead of over the number of ensemble members. The skill (in %) is then calculated by:

$$Skill = \frac{RMSD_{CTRL} - RMSD}{RMSD_{CTRL}} \cdot 100 \quad (4)$$

where CTRL denotes the ensemble simulation without any data assimilation (noDA). RMSD and skill are typical measures for
 160 the quality of a simulation that are commonly used in Numerical Weather Prediction (NWP, e. g. Bauer et al. (2015))

2.4 IsoGSM output and derived parameters

For the assessment of the assimilation experiments we use the IsoGSM output of the following parameters: temperature (T), zonal (u) and meridional wind (v), vertical velocity (ω), specific humidity (q) and precipitation. The water isotopologues δD and $\delta^{18}O$ are derived from converting the model output of HDO and $H_2^{18}O$ from mixing ratios to the delta notation in per mille.
 165 The ratio R between the isotopologues HDO and H_2O is given in the δ notation and δD is then calculated with reference to the Vienna Standard Mean Ocean Water R_s ($\delta D = 1000 \times (R/R_s - 1)$ in ‰, with $R_s = 3.1152 \times 10^{-4}$). The apparent heat flux of the large scale motion system Q_1 and the apparent moisture sink Q_2 which is due to the net condensation and vertical divergence of the vertical eddy transport of moisture are calculated based on the equations given in Yanai et al. (1973).

$$Q_1 = \frac{\partial s}{\partial t} + \mathbf{V} \cdot \nabla s + s \frac{\partial q}{\partial p} \quad (5)$$

170

$$Q_2 = -L \left(\frac{\partial q}{\partial t} + \mathbf{V} \cdot \nabla q + \omega \frac{\partial q}{\partial p} \right) \quad (6)$$

where s is the dry static energy, ω the vertical velocity, L is the latent heat of net condensation, q the specific humidity, \mathbf{V} the horizontal wind vector and p the pressure.



3 Results

3.1 Assessment of the performance in the tropics

The assessment is performed for the tropics in the latitude range from 10°S to 10°N and for the one month period of August 2016. We focus on the region in the tropics where heating is strong and where the Walker circulation is prevailing. Qualitatively the same results as the ones presented here are derived when the latitude band 20°S to 20°N, 20°S to 0° or 0° to 20°N is considered.

In the following this experiment is called “noDAvsDA” and consists of three assimilation runs and one ensemble run without any data assimilation (see Tab. 1). The assimilation run where only δD is assimilated is called IASI δD , the one with the assimilation of water vapour data is called IASI q and the one with assimilation of both, δD and q , is called IASI $\delta D+q$. These three assimilation experiments are then compared to an IsoGSM ensemble simulation without any data assimilation (called noDA). The following nine parameters are assessed: zonal and meridional wind (u, v), vertical velocity (ω), temperature (T), specific humidity (q), the isotopologues (δD and $\delta^{18}O$), heat source (Q_1) and moisture sink (Q_2).

Figure 1 (left) shows the spatial and temporal averaged vertical profiles of the RMSD for the tropics (one month average over all longitudes) of all nine parameters considered in this study. For all parameters the RMSD is reduced throughout the troposphere when δD is assimilated. A higher reduction can be derived when H_2O is assimilated instead of δD . The highest reduction in the RMSD, however, is found when both δD and H_2O are assimilated.

In Fig. 2 the corresponding profiles of the skill for the three assimilation runs are shown. For most parameters considered here the skill profiles reach a maximum at about 500-600 hPa which corresponds to the altitude where the IASI data has been assimilated. For the assimilation run with the assimilation of δD only positive values are found throughout the troposphere for almost all parameters indicating an improvement. Only for ω , Q_1 and Q_2 (Fig 2c, h, i) slightly negative values are found which indicate a slight degradation for these parameters. This degradation is mainly restricted to the lowest or highest pressure levels (above 150-200 hPa and for Q_1 below 700 hPa, Q_2 below 500 hPa and ω below 800 hPa). Inbetween, thus in the free troposphere, the assimilation of δD has either no impact (skill around 0 %) or causes a slight degradation. Only for Q_2 a slight improvement can be derived in the mid-troposphere (at about 200-400 hPa).

If however H_2O is assimilated (IASI q) instead of δD or if δD is assimilated together with H_2O (IASI $\delta D+q$) also ω , Q_1 and Q_2 can be improved. Thereby, higher positive skills are found for the assimilation of water vapour than for the assimilation of δD alone (Fig 2c, h, i). This is not surprising since water vapour has tighter direct connections to atmospheric dynamics and thermodynamics than δD (Field et al., 2014; Stevens et al., 2017). The highest skills are, however, obtained when δD is assimilated additionally to water vapour confirming that water isotopologues hold different aspects of information than water vapour (Galewsky and Hurley, 2010; Yoshimura et al., 2011; Noone, 2012).

Figure 3 shows bar charts of the skill for the noDAvsDA experiment for the tropics derived from the vertical profiles (for the troposphere, up to the 100 hPa level) for the month August 2016. Thus, this bar charts provide the average performance over the troposphere and thus summarizes our results. For all three assimilation runs the highest improvement is found for the zonal wind u and the lowest for ω , Q_1 and Q_2 . As was already visible in the profiles (Fig. 2) an improvement is found in the

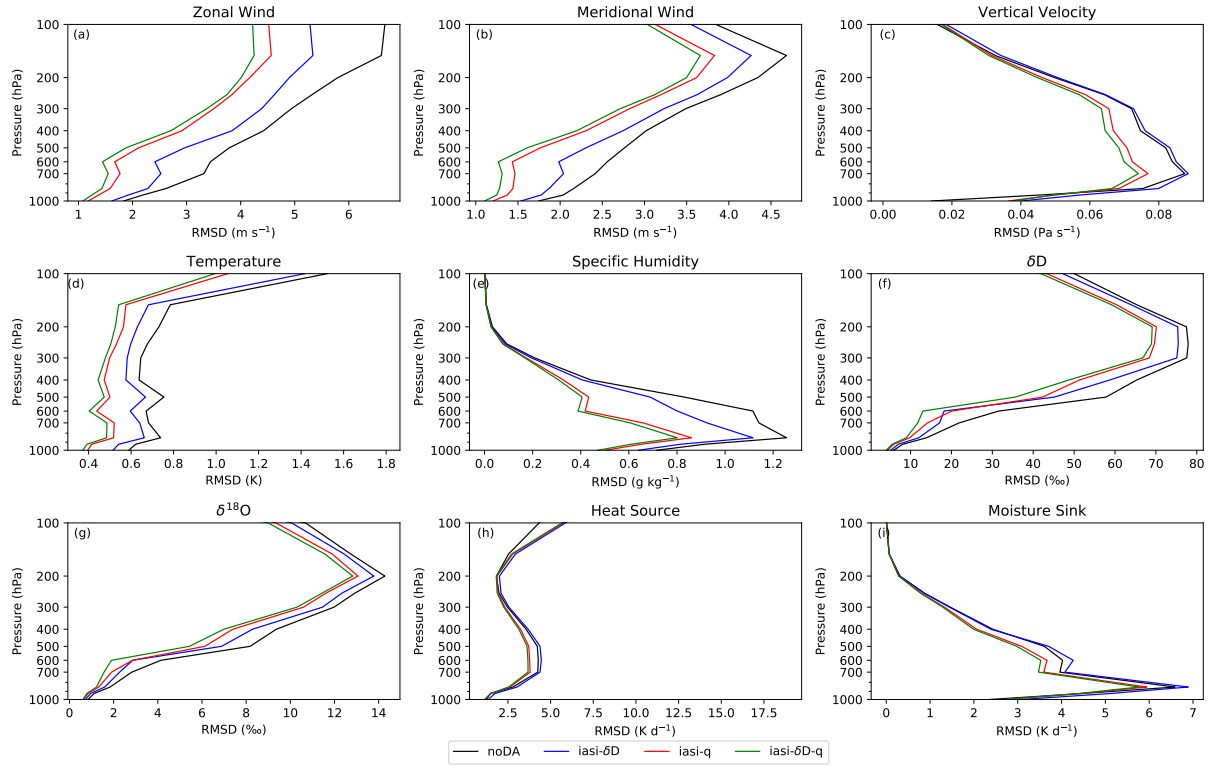


Figure 1. Spatial and temporal averaged vertical mean profiles of the RMSD for the ensemble simulation without any data assimilation - noDA (black), the assimilation with the mocked IASI δD data - IASI δD (blue), the mocked IASI H_2O data - IASI q (red), and the assimilation of both, H_2O and δD - IASI $\delta D+q$ (green), for the tropics ($10^\circ S$ to $10^\circ N$) for August 2016. Shown are all nine parameters considered in this study.

tropical troposphere for all parameters except ω , Q_1 and Q_2 when only δD is assimilated. For these three parameters a slight degradation (-5% for ω , -7% for Q_1 and -3% for Q_2) is found. The improvement for the other parameters is in the range of 11-17% (Fig. 3).

When only water vapour is assimilated an improvement of 5-7% for ω , Q_1 and Q_2 can be derived and between 20-36% for the other parameters. Even higher improvements are derived when δD is assimilated additionally to water vapour. Here, the improvements range between 8 and 10% for ω , Q_1 and Q_2 and between 27-41% for the other parameters.

3.2 Assessment of the performance in the tropics by specific regions

Figure 4 shows the longitude-pressure cross sections for Q_1 , Q_2 and ω for the tropics (monthly mean for August 2016). The longitudinal distribution is strongly tied to the equatorial Walker circulation which consists of several east–west circulation cells spanning different longitudinal sectors along the Equator. The major cell of the Walker circulation is located above the tropical Pacific (Peixoto and Oort, 1992). Regions of enhanced diabatic heating (Fig. 4) are found in the convective regions

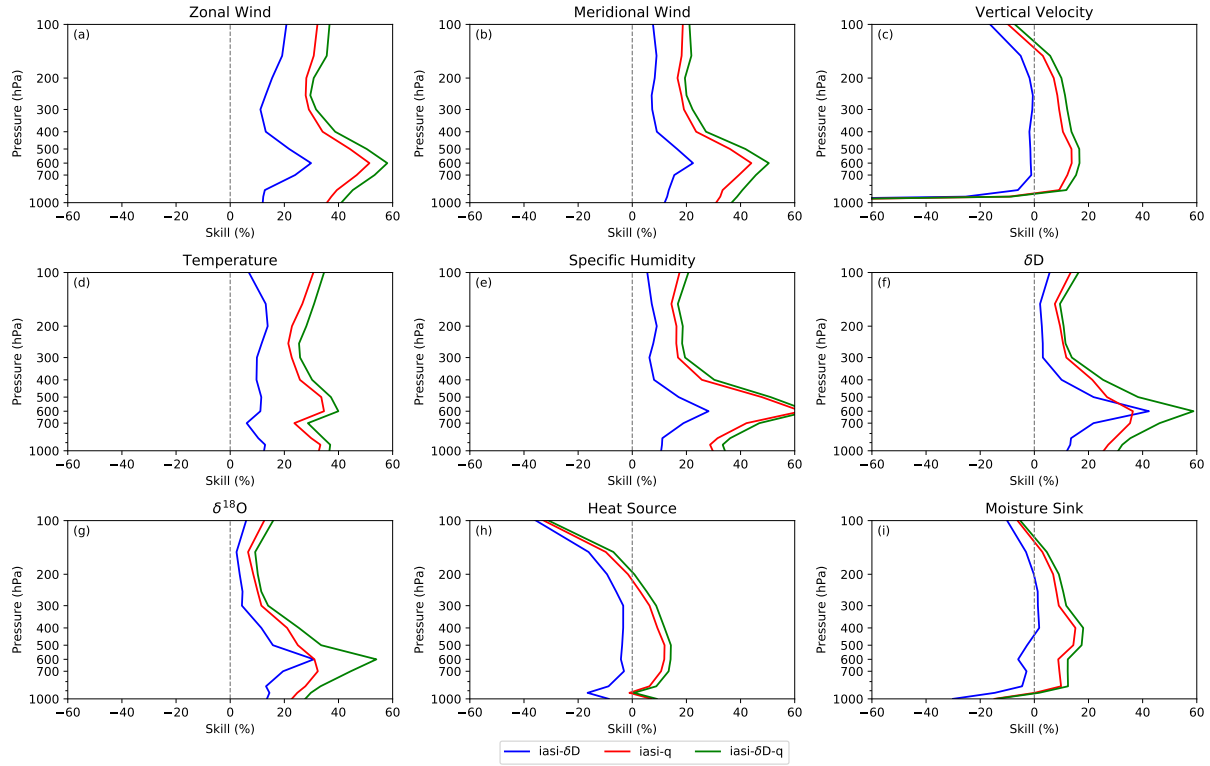


Figure 2. Spatial and temporal averaged vertical mean profiles of the skill for the assimilation with the mocked IASI δD data - IASI δD (blue), the mocked IASI H_2O data - IASI q (red), and the assimilation of both, H_2O and δD - IASI $\delta D+q$ (green), for the tropics ($10^\circ S$ to $10^\circ N$) for August 2016. Shown are all nine parameters considered in this study.

over Asia (around $120^\circ E$), South America (around $60^\circ W$) and western and central Africa (near $20^\circ E$). Conversely, the strong
 220 subsidence over the eastern Pacific leads to the absence of convection (Takayabu et al., 2010; Wright and Fueglistaler, 2013).

In Khosrawi et al. (2021) we found high RMSDs of δD and Q_2 in the regions where the upward and downward branches
 of the atmospheric circulation are located when IASI δD is assimilated additional to conventional observations. Thereby, we
 found that these regions of high RMSD in δD coincide with regions where strong upward/downward motion and diabatic heat-
 ing/cooling is dominant while for Q_2 these regions coincide with the regions where upward motion and heating is dominant.
 225 Further, Toride et al. (2021) found that the assimilation of water isotopologues additional to conventional observations can
 improve atmospheric circulation.

To investigate the relationship between the assimilation of water vapour and water vapour isotopologues and atmospheric
 circulation further, we made a separation into upward and downward branches and investigate the improvement in skill in
 these regions when IASI δD , IASI q or both is assimilated (Fig. 5). To this end, we selected in east-west direction four upward
 230 branches (Up America ($30^\circ W$ – $80^\circ W$), Up Africa ($0^\circ E$ – $50^\circ E$), Up West Pacific ($150^\circ E$ – $150^\circ W$) and Up Asia ($70^\circ E$ – $120^\circ E$))

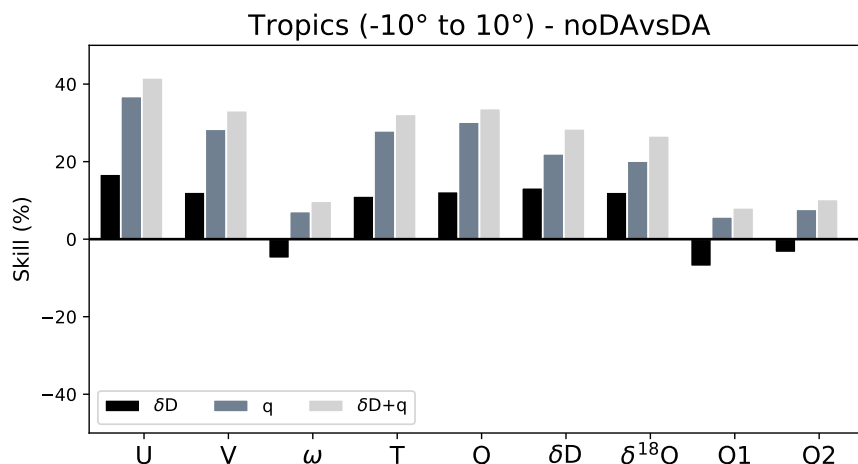


Figure 3. Improvement/degradation in skill in percent for each parameter in the troposphere (up to the 100 hPa level) derived from the vertical mean profiles in the tropics assimilating the mocked IASI δD - IASI δD (black), IASI H_2O - IASI q (dark grey) and both, IASI δD and H_2O data - IASI $\delta D+q$ (light grey).

and two downward branches (Down West Pacific (100°E–170°E) and Down Atlantic (50°W–10°E)) as indicated in Fig. 4 bottom panel.

Figure 5 summarizes the results for all parameters for the three assimilation experiments for the troposphere (averaging the spatial and temporal mean skill profiles up to 100 hPa). We generally find, in agreement with Toride et al. (2021), an improvement in the atmospheric circulation when δD is assimilated. However, we do not see from the analyses performed here a general better performance on either upward or downward branches. An exception are here ω , Q_1 and Q_2 for which better results are derived for the upward than for the downward branches. The degradation in the upward branches is much lower than for the downward branches and can be turned into an improvement when water vapour or water vapour together with isotopologues are assimilated (Figure 5 middle and bottom).

In the assimilation run with δD only, the degradation for ω , Q_1 and Q_2 is about -2 to -8% for the upward branches and about -7% to -28% for the downward branches. An exception is, however, Q_2 for Up America, where a slight improvement is found which, however, is so small that the bar is hardly visible in the figure. For the assimilation run with water vapour only an improvement in ω , Q_1 and Q_2 is derived for all upward branches and while for the downward branches still a degradation is found, except for ω and Q_2 in the Down Atlantic branch where a slight improvement is derived.

Although the improvement is generally higher for the assimilation of both, δD and H_2O than for the assimilation of water vapour alone, still a degradation in the Down West Pacific branch remains for ω , Q_1 and Q_2 . Nevertheless, the degradation is lower than for the assimilation with water vapour alone. Thus, the additional assimilation of δD leads to a general improvement and thus to a reduction of the degradation of ω , Q_1 and Q_2 . How large actually the additional gain from the δD is, will be assessed in the next Section.

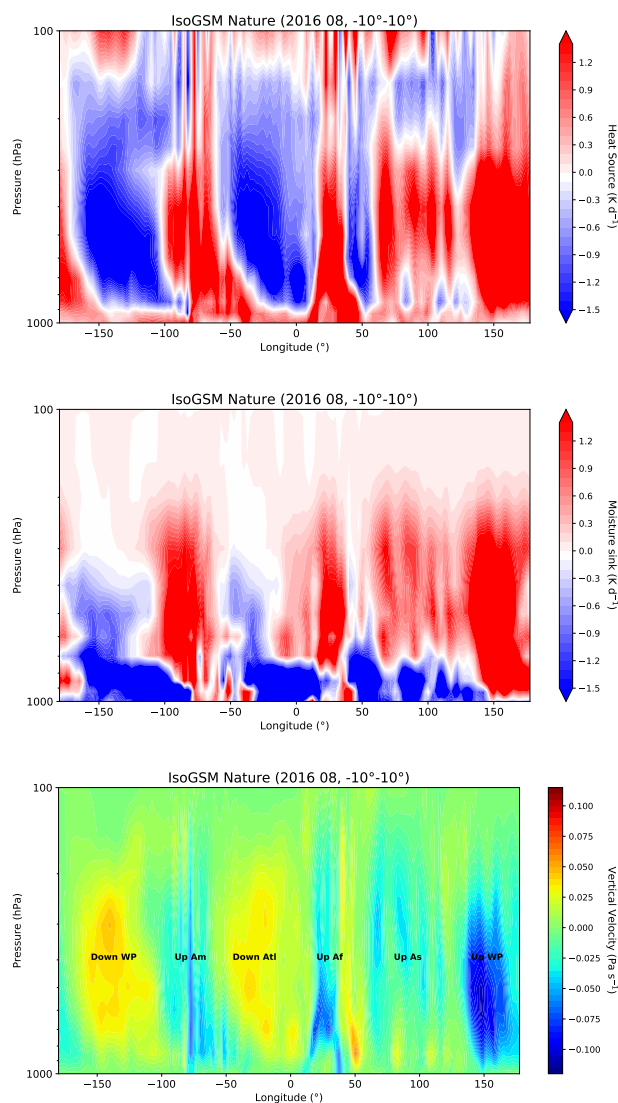


Figure 4. Longitude-pressure cross sections for heat source (Q_1), moisture sink (Q_2) and vertical velocity (ω) derived from the Nature run for the tropics (from top to bottom) for August 2016 (10°S to 10°N).

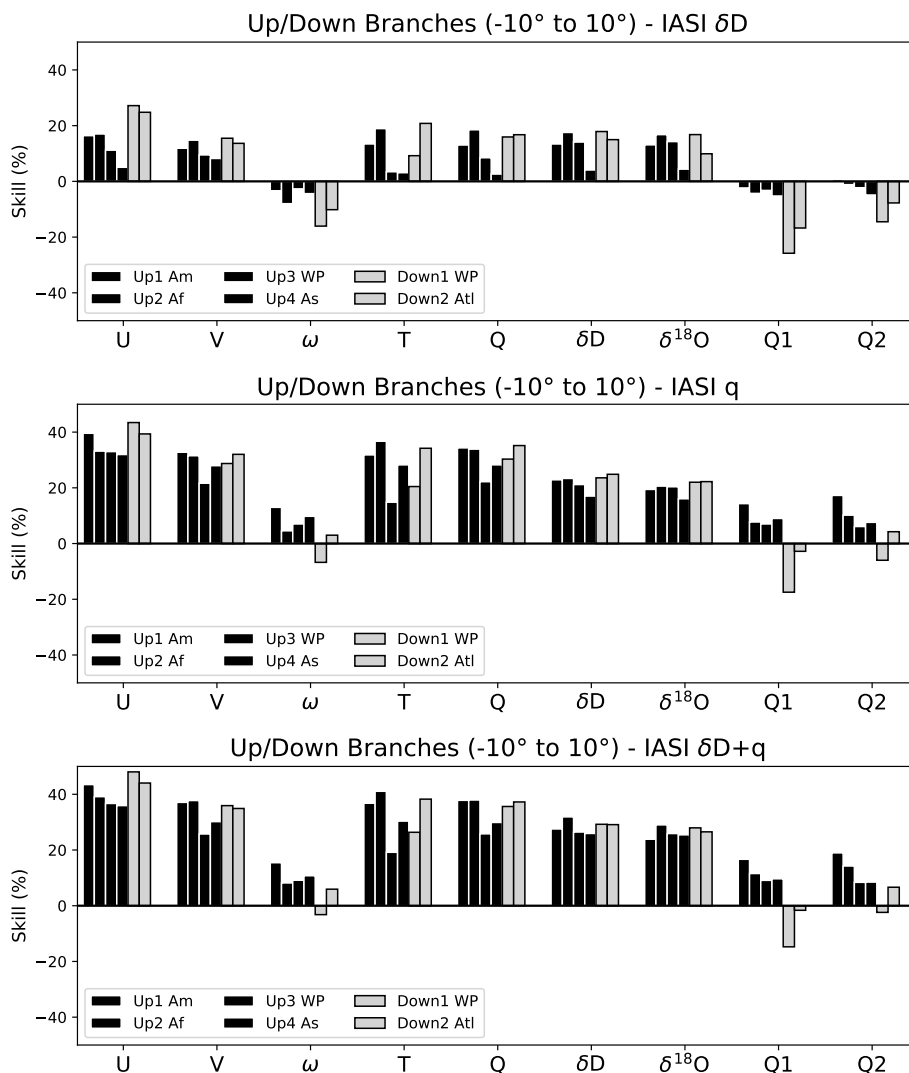


Figure 5. Improvement/degradation in skill in percent for each parameter in the troposphere (up to the 100 hPa level) derived from the vertical mean profiles and separated into upward and downward branches. The top panel shows the results for the assimilation run with the assimilation of δD alone (IASI δD), the middle panel shows the results for the assimilation run assimilating the IASI H_2O data (IASI q) and the bottom panel the results for the assimilation run assimilating both δD and q (IASI $\delta D+q$).

250 3.3 Assessment of the additional gain from the isotopologues

The assimilation experiments using δD and water vapour alone show that the assimilation of δD alone already leads to an improvement but higher improvements are derived when water vapour instead of the δD is assimilated. The largest improvement, however, is derived when δD and water vapour are assimilated together. In the following we assess the additional gain from the δD and thus use the assimilation run with the assimilation of water vapour (IASI q) as reference.

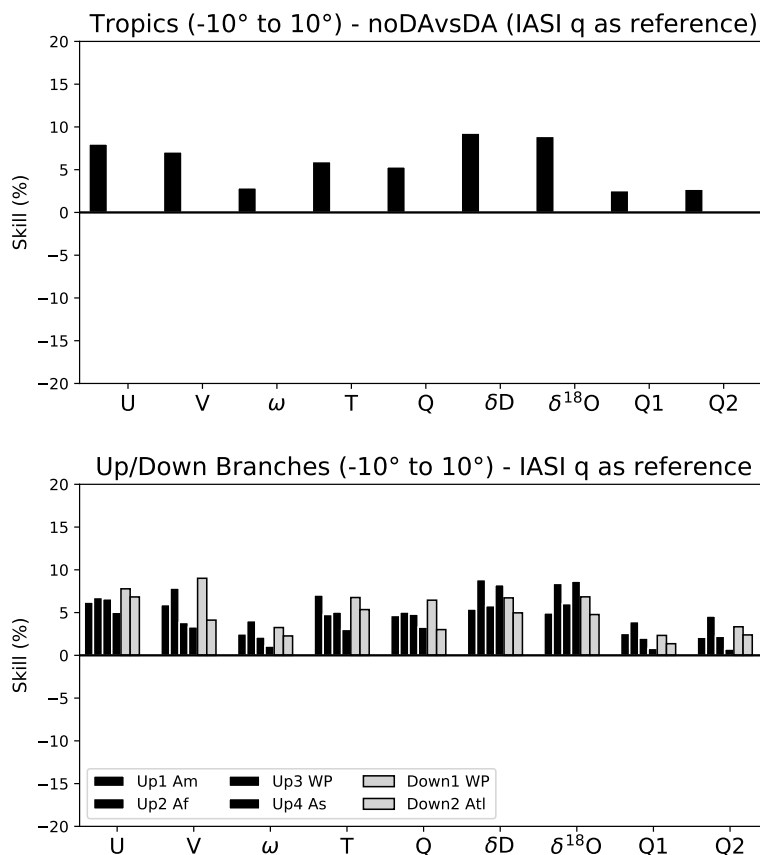


Figure 6. Improvement/degradation in skill in percent for each parameter in the troposphere (up to the 100 hPa level) derived from the vertical mean profiles. Here, the assimilation run IASI q has been used as reference to derive the additional gain when δD is assimilated additional to water vapour.

255 Figure 6 (top) shows the improvement in skill for each parameter in percent for the troposphere (up to the 100 hPa level) derived from the vertical mean profiles for the tropics. For all parameters an improvement is found when additionally to water vapour isotopologues are assimilated. The additional gain due to δD is in the range of 2-9%. Thereby the lowest improvement is with 2-3% found for ω , Q_1 and Q_2 and the highest for all other parameters with 5-9%.

260 The bottom panel of Fig. 6 shows the same as the top panel, but separated by the upward and downward branches. Also here, for all parameters an additional gain of 1-9% is found (1-5% for ω , Q_1 , Q_2 and 3-9% for all other parameters). Note, that here an improvement is also found for ω , Q_1 and Q_2 showing that the additional assimilation of δD at least helps to reduce the degradation that is found for these parameters in the downward branches and that still remains for the downward branches even when both, water vapour and δD are assimilated (Fig. 5). This degradation can only be turned into an improvement when additional conventional observations are assimilated (Khosrawi et al., 2021).

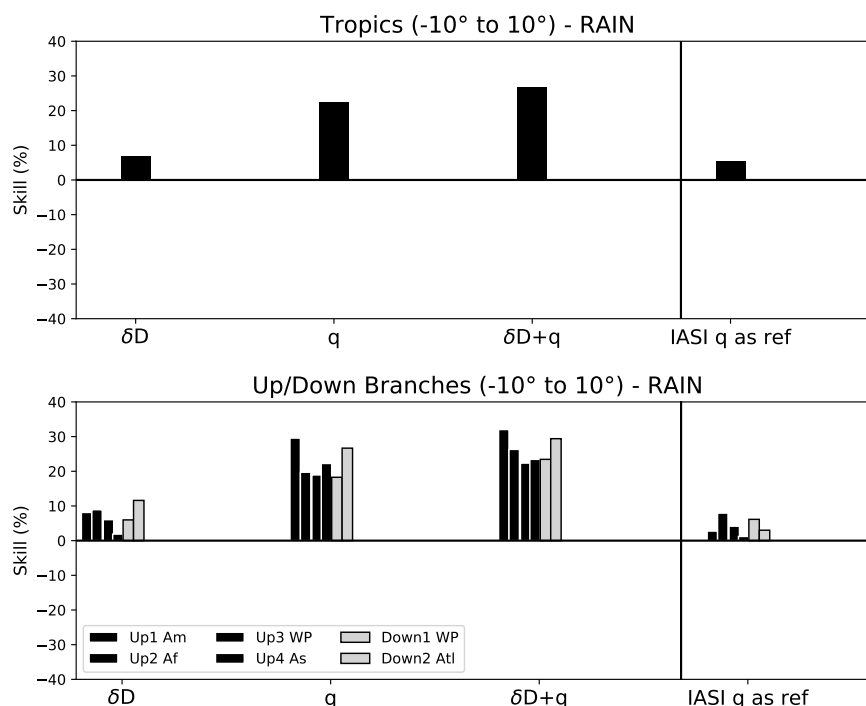


Figure 7. Improvement in skill in percent for precipitation for the assimilation run with δD only (IASI δD), with the assimilation of H_2O only (IASI q), the assimilation run with the assimilation of both δD and H_2O (IASI $\delta D+q$) and the improvement due to δD when IASI q is used as reference. Top: Tropics, bottom: Separated by upward and downward branches.

Further, there are differences in the performance dependent on which upward or downward branch is considered. For example, the highest gain from the additional δD assimilation is derived for Up Africa and Down West Pacific, while the lowest gain is found for Up Asia, except for the isotopologues δD and $\delta^{18}O$ for which a rather high improvement due to the additional δD assimilation is found.

3.4 Assessment of the performance for precipitation

In the following an overview of the performance of the assimilation experiments on the quality of precipitation in the meteorological analyses will be given. Figure 7 summarises the results of the three assimilation runs and when IASI q is used as a reference, for the entire tropics and separated into the upward and downward branches.

The same behaviour of the assimilation runs as for the other meteorological variables, discussed in the previous sections, is also found for precipitation irrespective if the entire tropics are considered or separated by longitude into upward and downward branches. The lowest improvements are found when only δD is assimilated, higher improvements are found for the assimilation of H_2O alone and the highest improvement is found when both δD and H_2O is assimilated together.

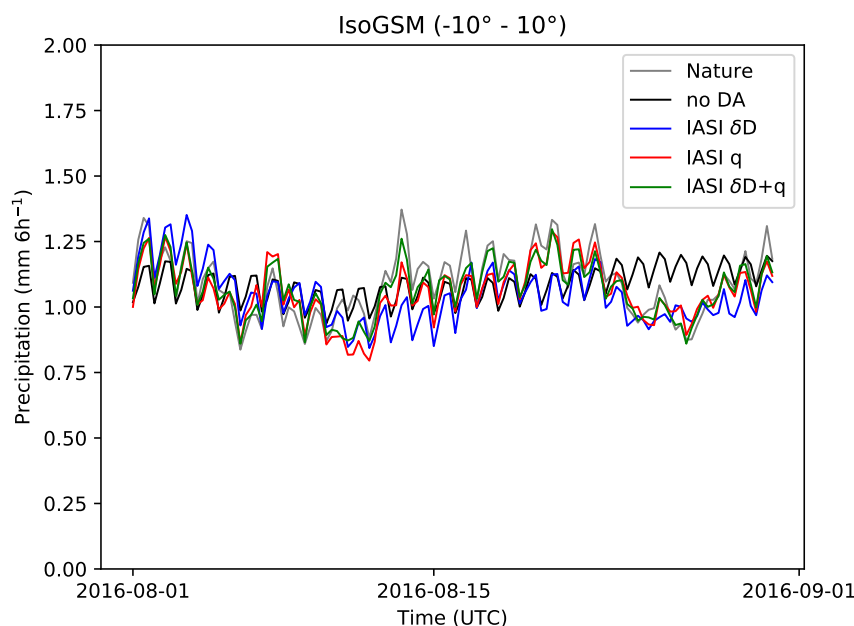


Figure 8. Time series of precipitation for the tropics (averaged over all longitudes for the latitude band 10° S to 10° N). Shown are the time series of the Nature (grey), the ensemble simulation without data assimilation noDA (black) and the three assimilation runs IASI δD (blue), IASI q (red), IASI $\delta D+q$ (green).

The improvements for precipitation in the tropics are as follows: 7% for the assimilation of δD only (IASI δD), 22% assimilation of H_2O only (IASI q) and 26% when both δD and H_2O are assimilated together (IASI $\delta D+q$). Separated by upward and downward branches the improvement is in the range of 2-12% for the assimilation of δD only (IASI δD), 19-30%
 280 for the assimilation of H_2O only (IASI q) and 23-32% when both δD and H_2O are assimilated together (IASI $\delta D+q$). The additional gain from the assimilation of δD compared to H_2O alone is 3-8% (IASI q as ref).

Figure 8 shows the time series of precipitation of the Nature, noDA, and the three assimilation runs averaged over the tropics (10° S to 10° N) for August 2016. The time series for noDA shows that this ensemble run solely simulates the climatological mean. When δD is assimilated the daily fluctuations that are missing in noDA are introduced, but still differences to the Nature
 285 remain. When water vapour is assimilated the daily fluctuations in the time series get already quite close to the Nature, but get even closer when both δD and water vapour are assimilated. This improvement in performance is also reflected in the Pearson correlation coefficient which is 0.33 for noDA, 0.60 for IASI δD , 0.79 for IASI q and 0.89 for IASI $\delta D+q$.

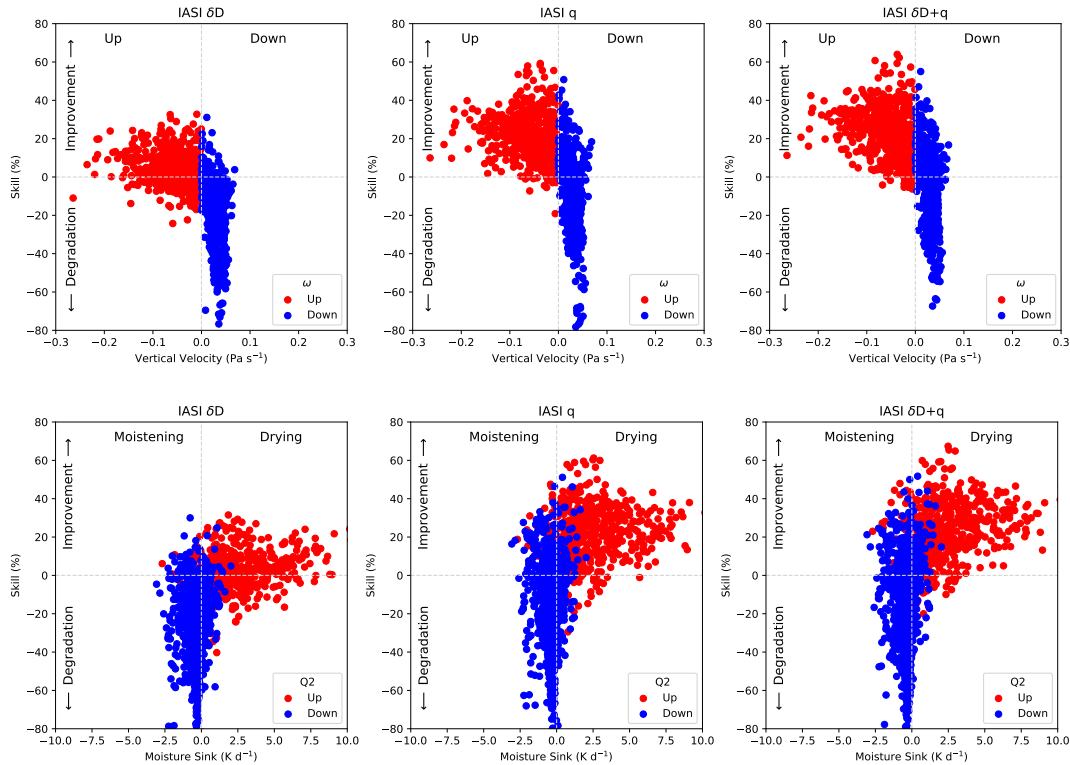


Figure 9. Correlation of the improvement/degradation in skill vs vertical velocity (top) and moisture sink (bottom) at 500 hPa for all lat/lon data points in the tropics (10° S to 10° N) separated by upward (red) and downward (blue) velocities.

4 Discussion

The assimilation experiments described in the previous sections show that the assimilation of δD has as water vapour the potential to improve the meteorological analysis in the tropics. Precipitation and all other meteorological variables except vertical velocity and the heating rates can be improved by 7-17%. However, heating rates (Q_1 and Q_2) and vertical velocity (ω) can only be improved in the tropics when either H_2O or both, δD and H_2O are assimilated (this study) or when additional to δD conventional observations are assimilated (Khosrawi et al. (2021)).

The separation in upward and downward branches shows that in the regions of downward motion still degradation remains, even when δD is assimilated together with H_2O . To investigate this further in the following correlation plots at 500 hPa are considered. Figure 9 shows the spatial correlations of vertical velocity and moisture sink, respectively, versus skill. Here, for the month August 2016 the data points for all latitude and longitude grid points at 500 hPa in the tropics between 10° S and 10° N are shown separated by vertical velocities into up and down, respectively. The correlation plots show that for the assimilation with δD mostly the data points with upward motion are improved while for the ones with downward motion mainly degradation is found. If water vapour alone or δD additionally to water vapour is assimilated a further improvement

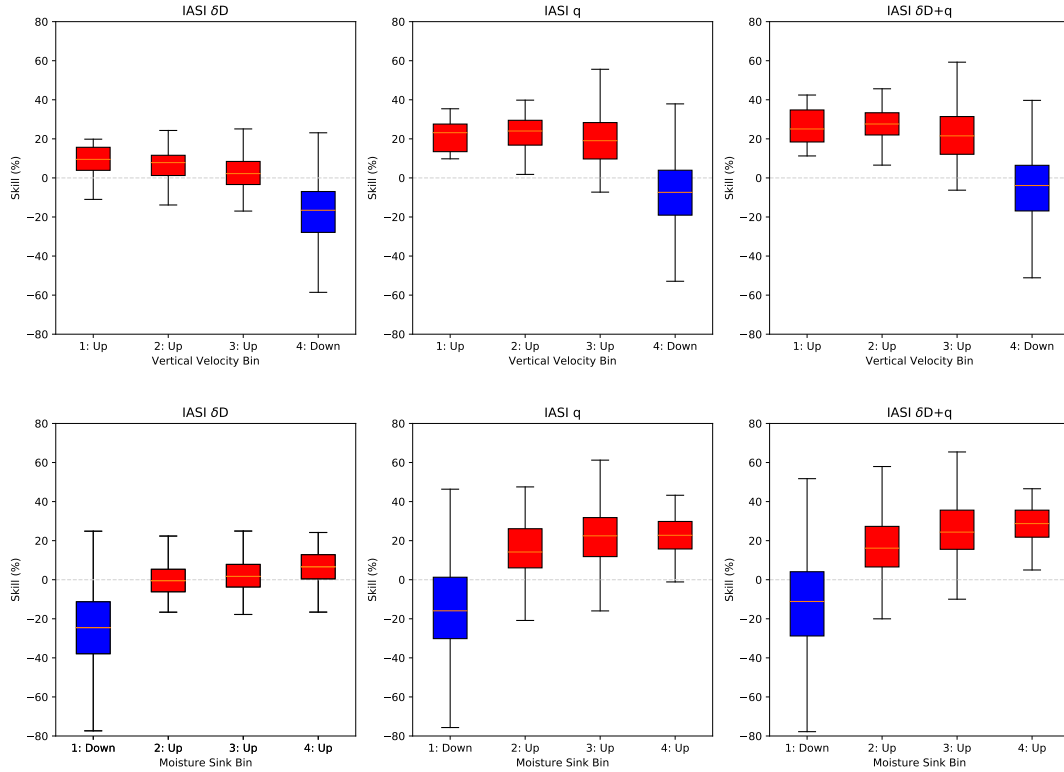


Figure 10. Box plot of the improvement/degradation in skill vs (top) vertical velocity (ω) and (bottom) moisture sink (Q_2) at 500 hPa for the tropics (10° S to 10° N) separated by upward (red) and downward (blue) velocities. The data has been separated into four bins (one for down, three for up) corresponding to the correlation plots shown in Fig. 9. The box covers the interquartile interval, where 50% of the data is found. The vertical line in the box is the median and the whiskers the maximum and minimum, respectively. Outliers are not shown.

is derived for the data points with upward motion so that almost all data points show an improvement. The degradation for the data points with downward motion still remains, but is significantly reduced when water vapour alone or δD additional to water vapour is assimilated. That a generally better performance of the assimilation is found for the upward branches than for the downward branches seems to be reasonable since there are less phase changes occurring in the downward branches than in

305 the upward branches (Toride et al., 2021).

The correlation plots show that as lower the vertical velocity (thus as higher the vertical updraft), as more positive skills (thus improvements) are found. To investigate that further we separate the data shown in the correlation plots into bins and present the results in a box plot using whiskers for each bin. Vertical velocity and moisture sink are therefore separated into the following four bins (three for upward motion and one for downward motion): ω Bin 1: -0.3 to -0.2 Pa s^{-1} , ω Bin 2: -0.2 to -0.1 Pa s^{-1} , ω Bin 3: -0.1 to 0 Pa s^{-1} , ω Bin 4: 0 to 0.1 Pa s^{-1} ; Q_2 Bin 1: -2.5 to 1.25 K d^{-1} (only down), Q_2 Bin 2: -2.5 to 1.25 K d^{-1} (only up), Q_2 Bin 3: 1.25 to 5.0 K d^{-1} , Q_2 Bin 4: $> 5.0 \text{ K d}^{-1}$.

310



As can be seen from the correlations shown in Fig. 9 and more obviously from the box plots shown in Fig. 10 is, that there is an increase in skill with increasing upward velocities and increasing (positive) moisture sinks, thus increasing latent heating. This behaviour is most pronounced in the assimilation run with δD (increase visible for both, ω and Q_2), but also visible in the other two assimilation runs (mainly for Q_2 and to some lesser extent for ω). Thus, this shows that δD has an higher impact in regions with strong updrafts where also stronger convection and thus more phase changes can be expected.

For the assimilation run with δD alone an increase in the median of ω (at 500 hPa) of about 7% is found, from 2.21 in Bin 3 (lowest upward velocities) to 9.49% in Bin 1 (highest upward velocities). For Q_2 the improvement is also 7%, from -0.48% in Bin 2 (for the lowest heating rates) to 6.62% for Bin 4 (the highest heating rates). Generally less degradation for the regions with downward motion and higher improvements for the regions with upward motion are found for the other two assimilation runs, but the increase in skill with increasing updraft velocities are somewhat lower (about 4%) and for the heating rates somewhat higher (8-12%) as for the assimilation run with δD only.

Considering the same scatter plots and box plot as shown in Figure 9 and Figure 10, respectively, but using the IASI q assimilation run as reference, shows that the assimilation of δD additional to water vapour lead also to a higher improvement in skill for upward than for downward motion (Figure 11 left). Further, the skill also improves with increasing strength of the upward velocities (Figure 11 right). However, in contrast to using the noDA assimilation run as reference, when additionally to water vapour isotopologues are assimilated, an improvement is found also for the bin covering the downward velocities. Thus, this means that here, both, upward and downward motion is improved i.e. atmospheric circulation, especially the upward/downward branches of the Walker circulation.

Fig. 12 shows the box plot for precipitation using the IASI q assimilation run as reference. Here, we use the following separation into five bins based on precipitation rate: One bin for “no rain” and four bins separating the data by increasing precipitation rate (Bin 1: $< 10 \text{ mm month}^{-1}$ (no rain), Bin 2: $10\text{-}250 \text{ mm month}^{-1}$, Bin 3: $250\text{-}500 \text{ mm month}^{-1}$, Bin 4: $500\text{-}750 \text{ mm month}^{-1}$, Bin 5: $> 750 \text{ mm month}^{-1}$). Fig. 12 shows that there is also an increase in improvement in precipitation with increasing precipitation rate when δD is assimilated additionally to water vapour. This is an important results since this shows that isotopes can help to improve the analyses especially in regions of heavy precipitation. Due to phase changing processes like rain condensation and evaporation and due to diffusive equilibration, precipitation is strongly tied to δD . Thus, in regions, where precipitation is strong, δD can provide supplementary information about the atmospheric state that cannot be obtained through H_2O alone (Worden et al., 2007; Risi et al., 2008; Torri et al., 2017).

5 Conclusions

In our study, we build on the study by Toride et al. (2021) and investigated which information is hold by the isotopologues. We were especially interested in answering the question if the information stored in the water isotopologues can improve diabatic heating rates and/or precipitation rates. Therefore, we performed idealized assimilation experiments where IASI data of δD , H_2O or both, δD and H_2O together, were mocked into an OSSE. In contrast to the assimilation experiments by Toride et al.

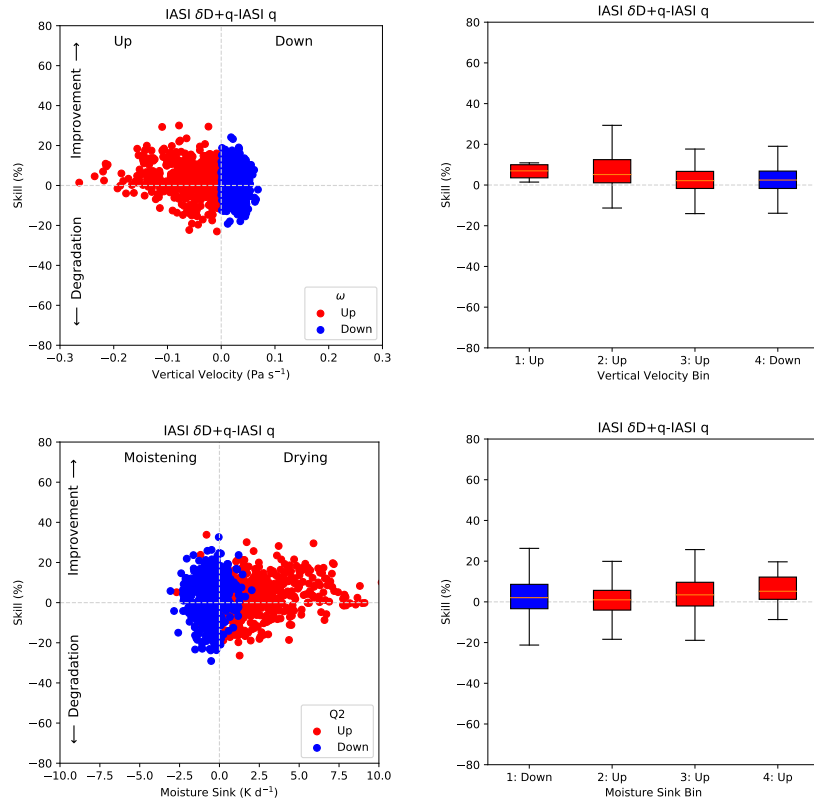


Figure 11. Left: Correlation of the improvement/degradation in skill vs vertical velocity ω (top left) and moisture sink Q_2 (bottom left) at 500 hPa for all lat/lon data points in the tropics (10° S to 10° N) separated by upward (red) and downward (blue) vertical velocities. Here, the IASI q assimilation run as is used as reference. Right: Box plot of the data shown on the left but separated into vertical velocity (top right) and moisture sink bins (bottom right). See text and Fig 10 for more details.

(2021) in our assimilation experiment no conventional observations were considered to be able to investigate the direct impact
 345 the water isotopologues have on the meteorological variables.

The assessment of the impact of this assimilation experiment on the meteorological analysis was performed for the tropics (10° S to 10° N). Thereby, additionally to the entire tropics also specific longitude regions in the tropics in east-west direction were considered that cover the upward and downward branches of the Walker circulation. To this end, we selected four upward branches (Up America (30° W– 80° W), Up Africa (0° E– 50° E), Up West Pacific (150° E– 150° W) and Up Asia (70° E– 120° E))
 350 and two downward branches (Down West Pacific (100° E– 170° E) and Down Atlantic (50° W– 10° E)).

The assimilation runs with the IASI data show that for all parameters the RMSD can be decreased and the skill improved when the mocked IASI data is assimilated. The highest improvement in skill and decrease in RMSD was generally found at ~ 500 – 600 hPa, the approximate altitude where the IASI data has the highest sensitivity and was assimilated into the IsoGSM model. Heating rates (Q_1 and Q_2) and vertical velocity (ω) can only be improved when either H_2O or δD , or δD and H_2O

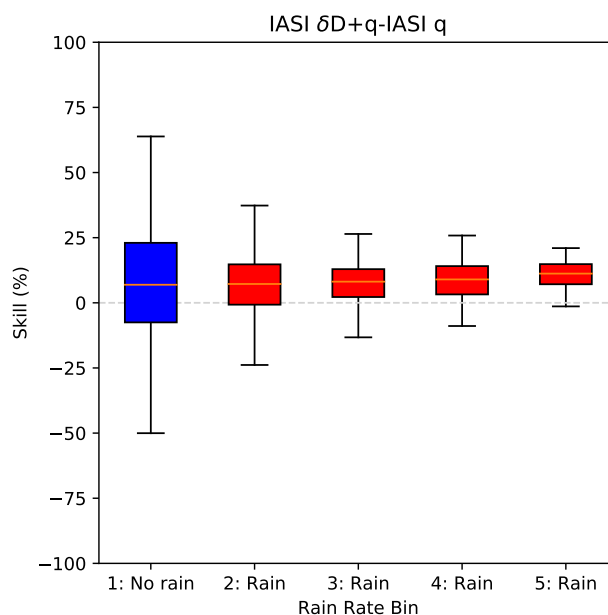


Figure 12. Box plot of the skill of rain separated into five bins, one bin for no rain and four bins based on the rain rate. See text for more details.

355 together, are assimilated. The assimilation of δD alone leads either to a slight improvement/degradation or no impact at all throughout the troposphere.

The improvements for all other parameters were higher for the assimilation of water vapour than for the assimilation of δD alone (IASI q or IASI δD) thus showing that the assimilation of H_2O is more efficient. However, the highest improvements were found for the assimilation run where δD and water vapour are assimilated together (IASI q+ δD) showing that the assimilation of both parameters is most efficient. Since changes in δD due to air parcel mixing are different from changes due to Rayleigh distillation at the same specific humidity (Galewsky and Hurley, 2010; Noone, 2012; Yoshimura et al., 2011), our results confirm that water isotopologues hold different aspects of information than water vapour.

Our study shows that the assimilation of IASI δD and/or H_2O data has the potential to improve meteorological analysis and thus also weather forecasts and climate predictions. More promising results in terms of improvement can be derived when IASI water vapour and/or δD are assimilated additional to conventional observations (Toride et al., 2021; Khosrawi et al., 2021). So far only idealized experiments were performed, but experiments with assimilating real IASI δD data are in progress. A first attempt of assimilating real IASI data (though an different data set than the one used here) was done by Tada et al. (2021). Based on a case study for a lower pressure system over Japan they could show that the assimilation of isotopologues leads to an improvement in forecast and analyses skill of a few percent. However, a lot of uncertainties concerning water isotope modelling and observations remain (Galewsky et al., 2016) that could hinder the realisation of the assimilation of real IASI data and/or compared to the idealised experiments lessen the impact of δD on the analysis fields (as discussed in Toride et al. (2021); Tada et al. (2021)). Nevertheless, in the future, when water vapour and isotopologues will be measured more frequently



together and the modelling of isotopic processes will be more accurate, the assimilation of isotopic observations additional to
water vapour may play an important role in improving the analysis and forecast skill because isotopologues provide unique
375 information relevant to atmospheric circulation and precipitation.

Data availability. The data for the noDAvsDA assimilation experiment can be obtained from the authors upon request. The MUSICA IASI
{H₂O,δD} pair data are publicly available from the RADAR4KIT repository (<https://dx.doi.org/10.35097/415>, Diekmann et al. (2021))

Author contributions. This study was designed by FK, MS, KY and KT. KY and KT performed the assimilation experiments. FK analysed
the assimilation experiments and wrote the manuscript with input from all co-authors. MS, CD, BE retrieved and provided the IASI data.

380 *Competing interests.* The authors declare that they have no conflict of interest.

Acknowledgements. This work was funded by the DFG project TEDDY (Project-ID: 416767181). The MUSICA IASI processing is per-
formed on the supercomputer ForHLR funded by the Ministry of Science, Research and the Arts Baden-Württemberg and by the German
Federal Ministry of Education and Research.

385 The article processing charges for this open-access publication were covered
by a Research Centre of the Helmholtz Association.



References

- Bauer, P., Thorpe, A., and Brunet, G.: The quiet revolution of numerical weather prediction, *Nature*, 525, 47–53, <https://doi.org/10.1038/nature14956>, 2015.
- 390 Bishop, C. H., Etherton, B. J., and Majumdar, S. J.: Adaptive sampling with ensemble transform Kalman filter. Part I: Theoretical Aspects, *Monthly Weather Review*, 128, 420 – 436, 2001.
- Chan, S. C. and Nigam, S.: Residual diagnosis of diabatic heating from ERA-40 and NCEP Reanalyses: Intercomparison to TRMM, *Journal of Climate*, 22, 414–428, <https://doi.org/10.1175/2008JCLI2417.1>, 2009.
- Clerbaux, C., Boynard, A., Clarisse, L., George, M., Hadji-Lazaro, J., Herbin, H., Hurtmans, D., Pommier, M., Razavi, A., Turquety, S.,
 395 Wespes, C., and Coheur, P.-F.: Monitoring of atmospheric composition using the thermal infrared IASI/MetOp sounder, *Atmospheric Chemistry and Physics*, 9, 6041–6054, <https://doi.org/10.5194/acp-9-6041-2009>, 2009, 2009.
- Dee, S. G., Nusbaumer, J., Bailey, A., Russell, J. M., Lee, J.-E., and Konecky, B.: Tracking the strength of the Walker circulation with stable isotopes in water vapor, *Journal of Geophysical Research*, 123, 7254–7270, <https://doi.org/10.1029/2017JD027915>, 2018.
- Diekmann, C. J., Schneider, M., Ertl, B., Hase, F., Garía, O., Khosrawi, F., Sepulvéda, E., Knippertz, P., and Braesicke, P.: The global and
 400 multi-annual MUSICA IASI {H₂O, δ D} pair dataset, *Earth System Science Data*, 13, 5273–5292, <https://doi.org/10.5194/essd-2021-87>, 2021.
- Field, R. D., Kim, D., LeGrande, A. N., Worden, J., Kelley, M., and Schmidt, G. A.: Evaluating climate model performance in the tropics with retrievals of water isotopic composition from Aura TES, *Geophysical Research Letters*, pp. 6030–6036, <https://doi.org/10.1002/2014GL060572>, 2014.
- 405 Frankenberg, C., Yoshimura, K., Warneke, T., Aben, I., Butz, A., Deutscher, N., Griffith, D., Hase, F., Notholt, J., Schneider, M., Schrijver, H., and Röckmann, T.: Dynamic processes governing lower-tropospheric HDO/H₂O ratios as observed from space and ground, *Science*, 325, 1374 – 1377, <https://doi.org/10.1126/science.1173791>, 2009.
- Galewsky, J. and Hurley, J. V.: An advection-condensation model for subtropical water isotopic ratios, *Journal of Geophysical Research*, 115, <https://doi.org/10.1029/2009JD013651>, 2010.
- 410 Galewsky, J., Steen-Larsen, H. C., Field, R. D., Worden, J., and Schneider, M.: Stable isotopes in atmospheric water vapour and applications to the hydrological cycle, *Reviews of Geophysics*, 54, 809–865, <https://doi.org/10.1003/2015RG000512>, 2016.
- González, Y., Schneider, M., Dyroff, C., Rodríguez, S., Christner, E., García, O. E., Cuevas, E., Bustos, J. J., Ramos, R., Guirado-Fuentes, C., Barthlott, S., Wiegeler, A., and Sepúlveda, E.: Detecting moisture transport pathways to the subtropical North Atlantic free troposphere using paired {H₂O- δ D} in situ measurements, *Atmospheric Chemistry and Physics*, 16, 4251 – 4269,
 415 <https://doi.org/https://doi.org/10.5194/acp-16-4251-2016>, 2016, 2016.
- Hunt, B. R., Kalnay, E., Kostelich, E. J., Ott, E., Patil, D. J., Sauer, T., Szunyogh, I., Yorke, J. A., and Zimin, A. V.: Four-dimensional ensemble Kalman filtering, *Tellus*, 56, 273–277, 2004.
- Hunt, B. R., Kostelich, E. J., and Szunyogh, I.: Efficient data assimilation for spatiotemporal chaos: A local ensemble transform Kalman filter, *Physica D*, 230, 112–126, 2007.
- 420 Kanamitsu, M., Kumar, A., Juang, H.-M. H., Schemm, J.-K., Wang, W., Yang, F., Hong, S.-Y., Peng, P., Chen, W., Moorthi, S., and Ji, M.: NCEP dynamical seasonal forecast system 2000, *Bulletin of the American Meteorological Society*, 83, 1019–1037, 2002.



- Khosrawi, F., Toride, K., Yoshimura, K., Diekmann, C. J., Ertl, B., Hase, F., and Schneider, M.: Can the assimilation of water isotopologue observation improve the quality of tropical diabatic heating and precipitation?, *Weather and Climate Dynamics Discussions*, <https://doi.org/10.5194/wcd-2021-49>, preprint, 2021.
- 425 Lacour, J.-L., Flamant, C., Risi, C., Clerbaux, C., and Coheur, P.-F.: Importance of the Saharan heat low in controlling the North Atlantic free tropospheric humidity budget deduced from IASI δD observations, *Atmospheric Chemistry and Physics*, 17, 9645–9663, <https://doi.org/10.5194/acp-17-9645-2017>, 2017.
- Lacour, J.-L., Risi, C., Worden, J., Clerbaux, C., and Coheur, P.-F.: Importance of depth and intensity of convection on the isotopic composition of water vapor as seen from IASI and TES δD observations, *Earth and Planetary Science Letters*, 481, 387–394, <https://doi.org/10.1016/j.epsl.2017.10.048>, 2018.
- 430 Lau, K.-M. and Yang, S.: Walker Circulation, in: *Encyclopedia of Atmospheric Sciences*, pp. 2505–2510, Academic Press, <https://doi.org/10.1016/B0-12-227090-8/00450-4>, 2003.
- Lee, J.-E., Fung, I., DePaolo, D. J., and Henning, C. C.: Analysis of the global distribution of water isotopes using the NCAR atmospheric general circulation model, *Journal of Geophysical Research*, 112, D16 306, <https://doi.org/doi:10.1029/2006JD007657>, 2017.
- 435 Ling, J. and Zhang, C.: Diabatic heating profiles in global reanalyses, *Journal of Climate*, 26, 3307–3325, <https://doi.org/10.1175/JCLI-D-12-00384.1>, 2013.
- Magnusson, L., Chen, J.-H., Lin, S.-J., Zhou, L., and Chen, X.: Dependence on initial conditions versus model formulations for medium-range forecast error variations, *Quarterly Journal of the Royal Meteorological Society*, 45, 2085–2100, <https://doi.org/10.1002/qj3445>, 2019.
- 440 Noone, D.: Pairing measurements of water vapour isotope ratio with humidity to deduce atmospheric moistening and dehydration in the tropical midtroposphere, *Journal of Climate*, 25, 4476–4494, <https://doi.org/10.1175/JCLI-D-11-00582.1>, 2012.
- Peixoto, J. P. and Oort, A. H.: *Physics of Climate*, American Institute of Physics, New York, USA, 1992.
- Risi, C., Bony, S., and Vimeux, F.: Influence of convective processes on the isotopic composition ($\delta^{18}O$ and δD) of precipitation and water vapor in the tropics: 2. Physical interpretation of the amount effect, *Journal of Geophysical Research*, 113, D19 306, <https://doi.org/10.1029/2008JD009943>, 2008.
- 445 Risi, C., Noone, D., Worden, J., Frankenberg, C., Stiller, G., Kiefer, M., Funke, B., Walker, K., Bernath, P., Schneider, M., Wunch, D., Sherlock, V., Deutscher, N., Griffith, D., Wennberg, P. O., Strong, K., Smale, D., Mahieu, E., Barthlott, S., Hase, F., García, O., Notholt, J., Warneke, T., Toon, G., Sayres, D., Bony, S., Lee, J., Brown, D., Uemura, R., and Sturm, C.: Process-evaluation of tropospheric humidity simulated by general circulation models using water vapor isotopologues: 1. Comparison between models and observations, *Journal of Geophysical Research*, 117, D05 303, <https://doi.org/10.1029/2011JD016621>, 2012.
- 450 Risi, C., Galewsky, J., Reverdin, G., and Briant, F.: Controls on the water vapor isotopic composition near the surface of tropical oceans and role of boundary layer mixing processes, *Atmospheric Chemistry and Physics*, 19, 12 235–12 260, <https://doi.org/10.5194/acp-19-12235-2019>, 2019.
- Risi, C., Muller, C., and Blossey, P.: What controls the water vapor isotopic composition near the surface of tropical oceans? Results from an analytical model constrained by large-eddy simulations, *Journal of Advances in Modeling Earth Systems*, 12, e2020MS002 106, <https://doi.org/10.1029/2020MS002106>, 2020.
- Schneider, A., Borsdorff, T., aan de Brugh, J., Lorente, A., Aemisegger, F., Noone, D., Henze, D., Kivi, R., and Landgraf, J.: Retrieving H_2O/HDO columns over cloudy and clear-sky scenes from the Tropospheric Monitoring Instrument (TROPOMI), *Atmospheric Measurement Techniques*, 15, 2251–2275, <https://doi.org/10.5194/amt-15-2251-2022>, 2022a.



- 460 Schneider, M. and Hase, F.: Optimal estimation of tropospheric H_2O and δD with IASI/METOP, *Atmospheric Chemistry and Physics*, 11, 11 207 – 11 220, <https://doi.org/10.5194/acp-11-11207-2011>, 2011.
- Schneider, M., Yoshimura, K., Hase, F., and Blumenstock, T.: The ground-based FTIR network's potential for investigating the atmospheric water cycle, *Atmospheric Chemistry and Physics*, 10, 3427 – 3442, 2010.
- Schneider, M., Wiegeler, A., Barthlott, S., González, Y., Christner, E., Dyroff, C., García, O. E., Hase, F., Blumenstock, T., Sepúlveda, E.,
 465 Mengistu Tsidu, G., Takele Kenea, S., Rodríguez, S., and Andrey, J.: Accomplishments of the MUSICA project to provide accurate, long-term, global and high-resolution observations of tropospheric $\{\text{H}_2\text{O}, \delta\text{D}\}$ pairs – a review, *Atmospheric Measurement Techniques*, 9, 2845 – 2875, <https://doi.org/10.5194/amt-9-2845-2016>, 2016.
- Schneider, M., Ertl, B., Diekmann, C. J., Khosrawi, F., Weber, A., Hase, F., Höpfner, M., García, O. E., Sepúlveda, E., and Kinnison, D.: Design and description of the MUSICA IASI full retrieval product, *Earth System Science Data*, 14, 709–742, <https://doi.org/10.5194/essd-14-709-2022>, 2022b.
 470
- Schrötte, J., Weissmann, M., Scheck, L., and Hutt, A.: Assimilating visible and infrared radiances in idealized simulations of deep convection, *Monthly Weather Review*, 148, 4357–4375, 2020.
- Stevens, B., Brogniez, H., Kiemle, C., Lacour, J.-L., Crovaisier, C., and Killiani, J.: Structure and dynamical influence of water vapour in the lower tropical troposphere, *SG*, 38, 1371–1397, <https://doi.org/10.1007/s10712-017-9420-8>, 2017.
- 475 Tada, M., Yoshimura, K., and Toride, K.: Improving weather forecasting by assimilation of water vapor isotopes, *Scientific Reports*, 11, <https://doi.org/10.1038/s41598-021-97476-0>, 2021.
- Takayabu, Y., Shige, S., Tao, W.-K., and Hirato, N.: Shallow and deep latent heating modes over tropical oceans observed with TRMM PR spectral latent heating data, *Journal of Climate*, 23, 2030–2046, <https://doi.org/10.1175/2009JCLI3110.1>, 2010.
- Toride, K., Yoshimura, K., Tada, M., Diekmann, C., Ertl, B., Khosrawi, F., and Schneider, M.: Potential of mid-tropospheric water vapor isotopes to improve large-scale circulation and weather predictability, *Geophysical Research Letters*, 48, e2020GL091698, <https://doi.org/10.1029/2020GL091698>, 2021.
 480
- Torri, G., Ma, D., and Kuang, Z.: Stable water isotopes and large-scale vertical motions in the tropics, *Journal of Geophysical Research*, 122, 3703–3717, <https://doi.org/10.1002/2016JD026154>, 2017.
- Uemura, R., Matusi, Y., Yoshimura, K., Motoyama, H., and Yoshida, N.: Evidence of deuterium excess in water vapor as an indicator of ocean surface conditions, *Journal of Geophysical Research*, 113, <https://doi.org/10.1029/2008JD010209>, 2008.
 485
- Webster, C. R. and Heymsfield, A. J.: Water isotope ratios D/H , $^{18}\text{O}/^{16}\text{O}$, $^{17}\text{O}/^{16}\text{O}$ in and out of clouds map dehydration pathways, *Science*, 302, 1742–1746, <https://doi.org/10.1126/science.1089496>, 2003.
- Webster, P. J. and Chang, H.-R.: Equatorial Energy Accumulation and Emanation Regions: Impacts of Zonally Varying Basic State, *Journal of the Atmospheric Sciences*, 45, 803–829, 1988.
- 490 Whitaker, J. S. and Hamill, T. M.: Evaluating methods to account for system errors in ensemble data assimilation, *Monthly Weather Review*, 140, 3078–3089, <https://doi.org/10.1175/MWR-D-11-00276.1>, 2012.
- Worden, J., Noone, D., Bowman, K., Beer, R., Eldering, A., Fisher, B., Gunson, M., Goldman, A., Herman, R., Kulawik, S. S., Lampel, M., Osterman, G., Rinsland, C., Rodgers, C., Sander, S., Shephard, M., Webster, C. R., and Worden, H.: Importance of rain evaporation and continental convection in the tropical water cycle, *Nature*, 445, 528 – 532, <https://doi.org/10.1038/nature05508>, 2007.
- 495 Worden, J. R., Kulawik, S. S., Fu, D., Payne, V. H., Lipton, A. E., Polonsky, I., He, Y., Cady-Pereira, K., Moncet, J.-L., Herman, R. L., Irion, F. W., and Bowman, K. W.: Characterization and evaluation of AIRS-based estimates of the deuterium content of water vapor, *Atmospheric Measurement Techniques*, 12, 2331–2339, <https://doi.org/10.5194/amt-12-2331-2019>, 2019.



- Wright, J. S. and Fueglistaler, S.: Large differences in reanalyses of diabatic heating in the tropical upper troposphere and lower stratosphere, *Atmospheric Chemistry and Physics*, 13, 9565 – 9576, <https://doi.org/10.5194/acp-13-9565-2013>, 2013.
- 500 Yanai, M., Esbensen, S., and Chu, J.-H.: Determination of bulk properties of tropical cloud clusters from large-scale heat and moisture budgets, *Journal of the Atmospheric Sciences*, 30, 611–627, 1973.
- Yoshimura, K., Oki, T., Ohte, N., and Kanae, S.: A quantitative analyses of short-term ^{18}O variability with a Rayleigh-type isotope circulation model, *Journal of Geophysical Research*, 108, 4647, <https://doi.org/doi:10.1029/2003JD003477>, 2003.
- Yoshimura, K., Oki, T., and Ichiyangi, K.: Evaluation of two-dimensional atmospheric water circulation fields in reanalyses by using
 505 precipitation isotopes databases, *Journal of Geophysical Research*, 109, <https://doi.org/10.1029/2004JD004764>, 2004.
- Yoshimura, K., Kanamitsu, M., Noone, D., and Oki, T.: Historical isotope simulation using reanalyses atmospheric data, *Journal of Geophysical Research*, 113, D19 108, <https://doi.org/10.1029/2008JD010074>, 2008.
- Yoshimura, K., Frankenberg, C., Lee, J., Kanamitsu, M., Worden, J., and Röckmann, T.: Comparison of an isotopic atmospheric general
 510 circulation model with new quasi-global satellite measurements of water vapor isotopologues, *Journal of Geophysical Research*, 116, <https://doi.org/10.1029/2011JD16035>, 2011.
- Yoshimura, K., Miyoshi, T., and Kanamitsu, M.: Observing system simulation experiments using water vapour isotope information, *Journal of Geophysical Research*, 119, 7842–7862, <https://doi.org/10.1002/2014JD021662>, 2014.